

Active Learning from Scene Embeddings for End-to-End Autonomous Driving

Wenhao Jiang¹, Duo Li², Menghan Hu¹, Chao Ma³, Ke Wang², Zhipeng Zhang²

¹Eact China Normal University, ²KargoBot, ³Shanghai Jiao Tong University

51255904051@stu.ecnu.edu.cn, {liduo, kewang}@kargobot.ai, mhu@ce.ecnu.edu.cn, chaoma@sjtu.edu.cn, zhipeng.zhang.cv@outlook.com

Abstract

In the field of autonomous driving, end-to-end deep learning models show great potential by learning driving decisions directly from sensor data. However, training these models requires large amounts of labeled data, which is time-consuming and expensive. Considering that the real-world driving data exhibits a long-tailed distribution where simple scenarios constitute a majority part of the data, we are thus inspired to identify the most challenging scenarios within it. Subsequently, we can efficiently improve the performance of the model by training with the selected data of the highest value. Prior research has focused on the selection of valuable data by empirically designed strategies. However, manually designed methods suffer from being less generalizable to new data distributions. Observing that the BEV (Bird’s Eye View) features in end-to-end models contain all the information required to represent the scenario, we propose an active learning framework that relies on these vectorized scene-level features, called *SEAD*. The framework selects initial data based on driving-environmental information and incremental data based on BEV features. Experiments show that we only need 30% of the nuScenes training data to achieve performance close to what can be achieved with the full dataset. Source code will be released.

1 Introduction

In recent years, deep learning has made breakthroughs across various fields [He *et al.*, 2016; Vaswani, 2017; Zhu *et al.*, 2020], with autonomous driving (AD) being one of the most promising areas of application. Early automated driving systems were primarily based on modular architectures, which relied on several independent subsystems to perform tasks such as perception, prediction, decision-making, and control [Behere and Törngren, 2015; Xu *et al.*, 2021]. While this approach has been successful to a certain extent, the subsystems need to manually design features and perform complex parameter tuning, which leads to high system development and maintenance costs and difficulty in handling complex and changing driving environments.

To overcome these limitations, end-to-end AD (E2E-AD) algorithms have gradually become a research hotspot [Hu *et al.*, 2022; Hu *et al.*, 2023; Jiang *et al.*, 2023]. E2E-AD integrates modules such as perceptual prediction planning into a pipeline, taking raw sensor data as input and directly outputting driving behavior. It realizes the fully differentiable learning of the whole process, eliminates the need for manual feature engineering and modular pipeline, and makes the system architecture more concise and efficient.

In complex and dynamic driving environments, E2E approaches demonstrate the potential to handle diverse scenarios and better tackle real-world challenges. However, E2E-AD models have higher data requirements [Caesar *et al.*, 2020; Jia *et al.*, 2024]. Training such models requires substantial scene data with detailed labeling information (e.g., 3D bounding boxes, segmentation masks), making data preparation a time-intensive and costly endeavor. To alleviate these labeling costs, active learning has emerged as a promising solution. By selecting the most informative samples for labeling, active learning aims to achieve high model performance with fewer labeled examples, thus reducing both labeling and training expenses [Ren *et al.*, 2021; Zhan *et al.*, 2022].

Currently, some studies are beginning to explore active learning methods in E2E-AD algorithms. For instance, [Lu *et al.*, 2024] introduces data selection strategies tailored to end-to-end scenarios with a focus on planning. However, their approach relies on the intermediate outputs of the model, e.g., the model’s perceptual ability, and action prediction ability. Some E2E models lack the computation of these intermediate quantities, which limits their ability to use this method. Besides, their scheme is artificially crafted and its robustness needs further experimental validation. Additionally, their data selection remains at the scene level, without exploring the feasibility of using more refined consecutive key frames.

There is an urgent need to find a data selection strategy that does not depend on manually set selection rules and is more generalizable to different data distributions. BEV algorithms [Phillion and Fidler, 2020; Huang *et al.*, 2021; Liu *et al.*, 2023] shine in AD by virtue of their ability to comprehensively perceive the environment, efficiently fuse multi-sensor data, and improve system stability and reliability. BevFormer [Li *et al.*, 2022] achieved state-of-the-art performance in perception tasks using solely visual inputs. As the latest

E2E-AD models increasingly rely on BEV features, filtering data within AD datasets based on BEV features presents a promising direction for future advancements.

Inspired by the above phenomenon, we propose an active learning method based on BEV features for E2E-AD. The BEV features are used to extract the scene-level embedding. Our method aligns with the standard active learning framework: initial training, data filtering, and retraining. We first leverage the abundant dynamic and static information in AD datasets to construct a diverse initial dataset, which is used to train a baseline model. Using this baseline model, we extract BEV features from the remaining data to evaluate scene value based on the predefined rule. The rule can be summarized as extracting key elements from BEV features and calculating the cumulative changes in these elements at the clip level as the selection criterion. For valuable scenes, key consecutive frames are selected and labeled, then combined with the existing data for further rounds of training and refinement.

We rigorously designed and conducted fair comparative experiments to validate the effectiveness of our proposed approach. The experimental results demonstrated a notable improvement in model planning performance, achieved under identical or even reduced labeling budgets. We further performed ablation studies to systematically examine the contribution of each individual module within our approach. Additionally, we included visualizations of selected frames to provide an intuitive understanding of the internal mechanics and impact of these modules. To comprehensively evaluate the robustness of our algorithm, we extended its application to multiple datasets, enabling us to verify its adaptability and stability across diverse data scenarios. Our principal contributions can be summarized as follows:

- We prioritized the selection of data with high utility for End-to-End Autonomous Driving (E2E-AD) from a Bird’s Eye View (BEV) perspective. This targeted data selection is instrumental in optimizing the performance of the E2E-AD system.
- Our approach achieved competitive performance while significantly reducing labeling requirements, demonstrating not only its efficiency but also its potential to address challenges in practical applications where labeling resources are limited or costly.
- We successfully extended our algorithm to a broader spectrum of models and datasets. This extension substantiates the robustness of our algorithm, demonstrating its capacity to deliver stable and reliable performance across various environments and frameworks.

2 Related Work

2.1 End-to-End Autonomous Driving

E2E-AD aims to cope with the risks of information loss, error accumulation, and feature misalignment that may result from the separation of traditional model modules [Chen *et al.*, 2024; Tampuu *et al.*, 2020; Hu *et al.*, 2023]. Current algorithms mainly follow the idea of imitation learning, i.e., training a model by mimicking the behavior of an expert. CILRS [Codevilla *et al.*, 2019] investigates the advantages

and limitations of imitation learning in E2E-AD and gives new benchmarks. LBC [Chen *et al.*, 2020] uses an agent model that has access to privileged information to guide the training of a purely visually based sensorimotor agent. Transfuser [Prakash *et al.*, 2021] and InterFuser [Shao *et al.*, 2023] propose the use of a sensor fusion Transformer, which combines the benefits of visual imagery and LiDAR to achieve advanced driving performance. ST-P3 [Hu *et al.*, 2022] uses a spatial-temporal feature learning scheme to achieve performance gains with purely vision-based inputs. UniAD [Hu *et al.*, 2023] designs an end-to-end autopilot framework that integrates full-stack tasks in a planning-oriented manner, jointly optimizing intermediate modules. VAD [Jiang *et al.*, 2023] uses vectorized scenario representations to improve model inference speed significantly. Some works use reinforcement learning ideas to train models [Zhang *et al.*, 2022; Kiran *et al.*, 2021]. [Toromanoff *et al.*, 2020; Chekroun *et al.*, 2023] use supervised learning to obtain a scene representation on which a shallow policy head is trained. [Knox *et al.*, 2023; Zhang *et al.*, 2021] design a reward function based on prior access to privileged information.

2.2 Active Learning

Active learning is a well-established approach that aims to minimize the annotation cost by selectively querying the most informative data points for labeling [Ren *et al.*, 2021; Zhan *et al.*, 2022]. Active learning algorithms primarily focus on uncertainty [Lewis and Catlett, 1994; Gao *et al.*, 2020; Joshi *et al.*, 2009] and data diversity [Sinha *et al.*, 2019; Agarwal *et al.*, 2020; Xie *et al.*, 2023]. Uncertainty-based methods prioritize the selection of samples with the highest uncertainty in model predictions, aiming to enhance the model’s generalization capability. Uncertainty can be measured through posterior probabilities [Lewis and Catlett, 1994], margin sampling [Roth and Small, 2006], or entropy [Joshi *et al.*, 2009]. Some studies leverage Bayesian inference, using techniques such as Monte Carlo Dropout [Gal and Ghahramani, 2016] or Deep Gaussian Processes [Damanou, 2015] to estimate predictive variance through multiple forward passes. Diversity-based strategies aim to select subsets of unlabeled data that comprehensively cover the data space, minimizing redundancy and enhancing generalization. Representative methods include clustering-based selection, core-set strategies [Sener and Savarese, 2017] that minimize the maximum distance between selected samples and the rest of the dataset, and submodular optimization [Elhamifar *et al.*, 2013] to select samples with the highest marginal gains. In addition to these, some algorithms assess the influence of data on the model [Liu *et al.*, 2021; Chhabra *et al.*, 2024]. ISAL[Liu *et al.*, 2021] proposes an approach to estimate the expected gradient of unlabeled samples, quantifying their potential impact on model performance and guiding the selection process accordingly. [Lu *et al.*, 2024] first combines active learning with E2E-AD, though their strategy’s generalizability requires further validation. Our approach offers a simple and efficient integration into BEV-based AD models.

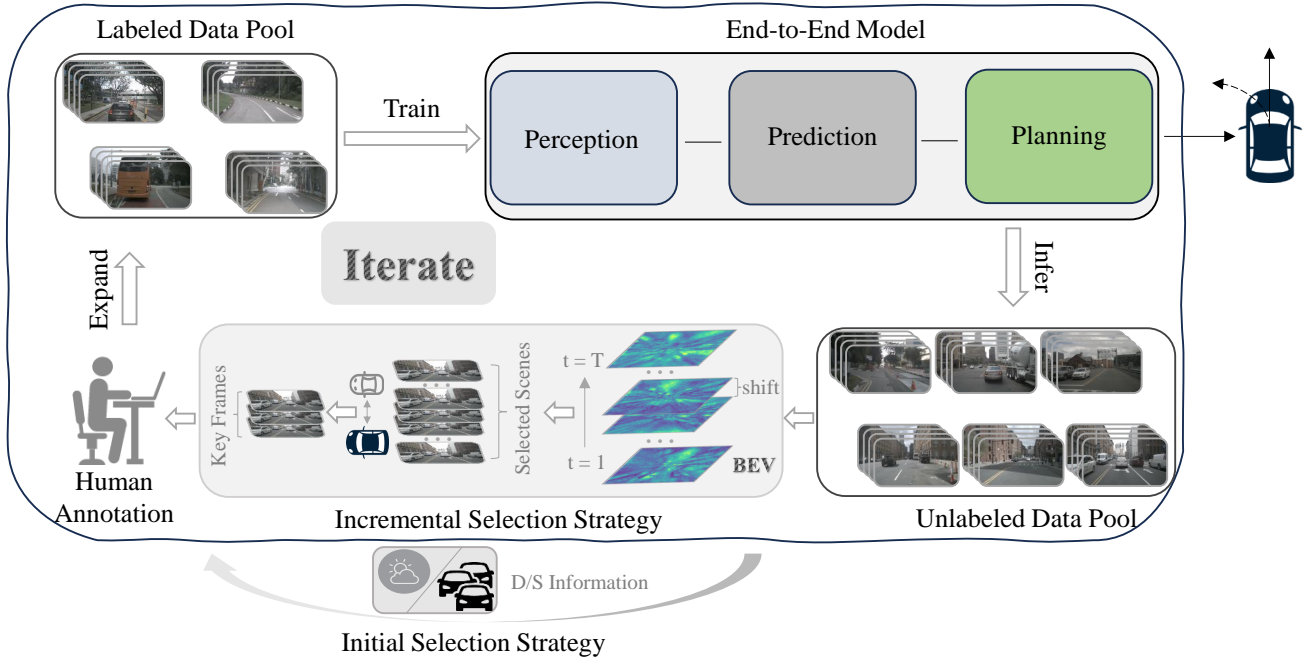


Figure 1: **Overall pipeline of SEAD.** Following the active learning setup, we first build an initial training set based on the initial strategy to train the model. Subsequently, we leverage the trained model and incremental selection strategy to actively select new data, iterating this process continuously. In this context, D/S represents dynamic/static.

3 Methods

3.1 Problem Definition

Our optimization objective for applying active learning to E2E-AD tasks is defined as $G = \text{Max}(\frac{P}{B})$, where P represents model planning performance and B denotes the labeling budget. This introduces two optimization strategies:

1. Given a target planning performance P , reduce the labeling budget B ;
2. Given a labeling budget B , improve the planning performance P .

In this paper, we adopt the second strategy.

Currently, commonly used AD datasets are structured at the clip-level. Specifically, the training set of a comprehensive AD dataset consists of N clips, each capturing a continuous driving scene over T frames. Within each clip, frames maintain contextual continuity with one another, making the use of clips as fundamental training units beneficial for tasks such as object tracking and route planning. Empirical evidence, as well as analysis of the data itself, reveals that corner cases represent only a small portion of all N clips. Furthermore, each clip may contain timestamped samples corresponding to repeated, simple scenarios.

We propose an active learning strategy designed to identify and extract valuable clips from the data pool, followed by the selection of key frames. Initially, given an available unlabeled data pool $P = \{x_i\}_{i \in [N]}$, we leverage the prior information within AD datasets to select valuable clip indices \mathcal{K} and construct the initial training set $\hat{P} = \{x_i, y_i\}_{i \in [\mathcal{K}]}$. The

model f is trained on \hat{P} . For incremental selection, f performs inference on the remaining data pool, with key frames selected according to predefined criteria. Combine selected key frames with \hat{P} for further training to update f . This incremental process is repeated until the total data reaches the budget B , depicted in Fig. 1.

3.2 Initial Dataset Construction Based on Dynamic and Static Information

In conventional active learning algorithms for general tasks (e.g., classification, object detection), a randomly selected subset of data is typically used to train the initial model. This approach is feasible because the data and labels in these tasks are relatively straightforward and lack additional contextual information. However, in autonomous driving (AD) tasks, a wealth of additional information is collected by the vehicle's sensors, such as lighting conditions, weather, speed, and cornering angle. This auxiliary information is readily available without extra labeling effort, allowing us to leverage it to construct an initial dataset that encompasses diverse scenarios. Following the structure of the nuScenes dataset [Caesar *et al.*, 2020], we build our initial dataset along two dimensions: static scene information and dynamic vehicle information, as illustrated in Fig. 2. Specifically, for static scene information, inspired by [Lu *et al.*, 2024], we categorize the training set into four subsets $\{DS, DR, NS, NR\}$ based on a combination of lighting conditions (day or night) and weather conditions (sunny or rainy).

Building on this, we further enhance the diversity by incorporating dynamic information gathered during vehicle

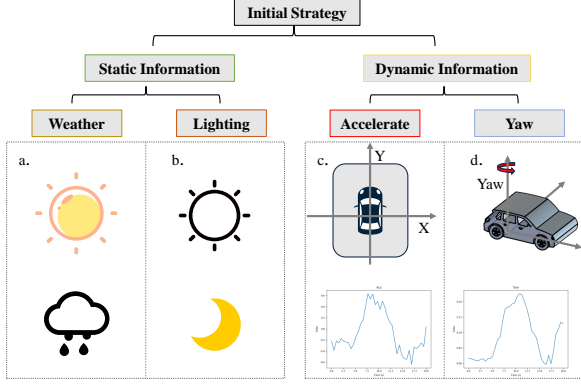


Figure 2: **Initial selection.** Constructing a diverse initial dataset by leveraging the rich information within the AD dataset.

motion. Information on vehicle acceleration and turning angle is available in the CAN bus data, from which we select the vehicle’s y -axis acceleration and yaw deflection.

Using these two parameters, we compute the standard deviation of acceleration and the cumulative turning angles within each scene to capture the dynamics of vehicle motion. After sorting based on these metrics, we obtain Acc and Yaw scores and apply a selection ratio, denoted as λ , to categorize the data into “valuable” and “normal” subsets. This results in four subsets: Acc_v , Acc_n , Yaw_v , and Yaw_n . The training set D_T is further divided into three subsets based on scene composition: scenes containing both Acc_v and Yaw_v , scenes containing only one, and scenes with neither.

$$\begin{aligned}
 B &= Acc_v \cap Yaw_v \\
 N &= Acc_n \cap Yaw_n \\
 S &= D_T - (B \cap N)
 \end{aligned} \tag{1}$$

Based on the static scene information and dynamic vehicle information, we can divide the whole training set into 12 subsets {DS-B, DS-S, DS-N, ..., NR-B, NR-S, NR-N} containing different driving behavior data in different scenes.

3.3 Key Scene-to-Frames based on BEV Features

In the initial selection phase, both static environmental and dynamic driving data were utilized. For incremental selection, the trained model was then used to extract dynamic and static information from the remaining data pool. We define dynamic information as the cumulative changes between frames throughout an entire scene, and static information as the interactions between scene participants within a specific frame. Based on these two types of information, we implemented a layered filtering process, progressing from the data pool to valuable scenes and subsequently to key frames.

Select Valuable Scenes Based on Dynamic Information

The model trained in the previous stage takes multi-view RGB images as input, and through a feature extraction module and a BEV encoder module, generates BEV features. A straightforward approach to measure changes between frames

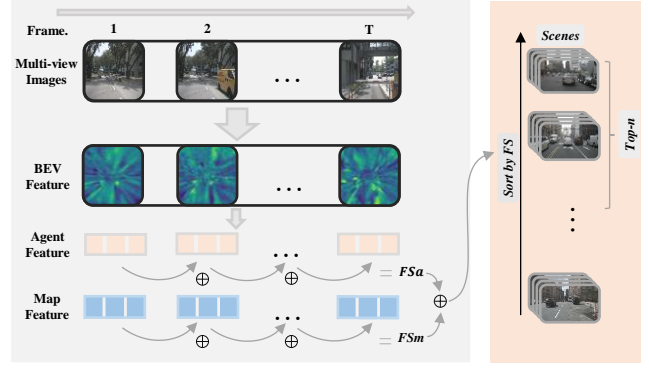


Figure 3: **Calculate FS for scenes.** Convert the computation of BEV FS to focus on the shifts of key elements, specifically the agent and map features. Then, accumulate the frame-to-frame FS results to determine the FS for the scene.

is to compute the feature shifts FS between two BEV representations. However, the high dimensionality of the BEV feature tensor makes direct computation time-intensive. Additionally, the richness of information within BEV feature maps could obscure the truly valuable parts. Given that the primary elements in road scenes are the map and agents, we can transform the task of computing FS between BEV frames into calculating the shifts in map and agent features specifically. This approach not only reduces computational demands but also concentrates on the information that is most relevant.

Taking agents as an example, the process is as follows: a query vector Q_a is constructed for the agent, with the previously obtained BEV features used as the value. Following the approach [Zhu *et al.*, 2020], this yields the agent’s feature representation F_a . In the clip-level data scenario, each scene contains T instances of F_a . The Earth Mover’s Distance (EMD) [Rubner *et al.*, 2000] is employed to measure the difference between two consecutive:

$$FS = EMD(F_{cur}, F_{prev}) \tag{2}$$

When the dimensionality of F_a is high, directly calculating the FS_a between two F_a becomes computationally expensive and resource-intensive. To reduce the computational complexity, we first apply a dimensionality reduction strategy to project F_a into a lower-dimensional space, denoted as F'_a , and then compute the FS_a between F'_a . The calculation process for the map is analogous, resulting in FS_m . The final FS_s of the scene is calculated as:

$$FS_s = \sum_{t=1}^T (FS_{a,t} + FS_{m,t}) \tag{3}$$

We select the top n clips with the largest FS_s from the data pool, where n represents the phase budget. The detailed process is illustrated in Fig. 3.

Select Key Frames Based on Static Information

When the distance between the ego vehicle and other road participants is large, the driving difficulty tends to be lower. From the perspective of interaction, we extract key

frames from a single clip. Assume a clip contains T frames, represented as $C_i = [f_1, f_2, \dots, f_T]$. For a specific frame f_k , after obtaining the queried feature F_a , a regression network is used for inference to provide predictions about the agent, including class, position, confidence, and other relevant information. By setting a confidence threshold θ_τ , targets with low confidence scores are filtered out, leaving the remaining targets with their corresponding positions $P = [p_1, p_2, \dots, p_n]$. The minimum distance between these remaining targets and the ego vehicle is then computed, and if this distance is smaller than the predefined distance threshold θ_d , the current frame is identified as a key frame:

$$y_k = \begin{cases} 1 & \text{if } \min_{i \in [1, n]} (p_{\text{ego}} - p_i) < \theta_d, \\ 0 & \text{otherwise.} \end{cases} \quad (4)$$

For each clip, we obtain an array $K = [y_1, y_2, \dots, y_T]$ of length T , which indicates whether each frame is a key frame. To ensure temporal continuity in the driving scenario, we select the longest sequence of consecutive key frames for subsequent annotation and training.

The workflow of the entire program is outlined in Alg. 1, covering both the initial selection and subsequent incremental selections. Given a total budget B , data samples are selected in batches of size n_{itr} at each iteration. The model is iteratively trained on all previously selected data, followed by a new data selection round, until the budget B is exhausted.

4 Experiments

4.1 Experimental Setup

We conduct experiments on nuScenes [Caesar *et al.*, 2020], a commonly used benchmark dataset for AD, with experimental settings aligned to previous work UniAD [Hu *et al.*, 2023], VAD [Jiang *et al.*, 2023].

Data/Metrics

The nuScenes dataset comprises a total of 1,000 diverse driving scenarios: 700 for training, 150 for validation, and 150 for testing, with each scenario lasting about 20 seconds. Data collection uses a vehicle outfitted with 6 cameras, 1 LiDAR, and 5 radars, offering a 360° horizontal field of view. Keyframes are annotated at a 2 Hz sampling rate, capturing comprehensive environmental details and vehicle driving behavior. We continue the setting of ActiveAD [Lu *et al.*, 2024] by setting a 30% annotation budget and selecting 10% of the data in each of the three batches.

The evaluation metrics employed in this study are aligned with the open-loop metrics of previous work [Hu *et al.*, 2022; Hu *et al.*, 2023; Jiang *et al.*, 2023], and displacement error (L2) and collision rate (CR) are chosen to measure the planning performance of the model.

Models/Training

We select VAD as our base model. Compared to previous works such as ST-P3 and UniAD, VAD leverages a vectorized scene representation to enable faster inference and improved open-loop performance. Additionally, the lightweight version, VAD-Tiny, requires less training time than the standard VAD-Base, with only minimal performance degradation. Therefore, we adopt VAD-Tiny for rapid solution validation.

Algorithm 1 Pseudo-code for SEAD

Require: Unlabeled pool $P = \{x_i\}_{i \in [N]}$, labeled pool $\hat{P} = \emptyset$, annotation budget B , iteration I , model f_{itr} , iterated selection n_{itr}

- 1: Selected clip index $\mathcal{K} = \emptyset$
- 2: **for** itr in range(I) **do**
- 3: **if** $itr == 0$ **then**
- 4: Calculate nums $\hat{n}_{x,y} = n_{itr} \times n_{x,y} / \sum_{x,y} n_{x,y}$, where $x \in \{\text{DS, DR, NS, NR}\}$, $y \in \{\text{B, S, N}\}$
- 5: Random select $\hat{n}_{x,y}$ samples in $P_{x,y}$ and add their indexes to \mathcal{K} .
- 6: Update $\hat{P} = \{x_i, y_i\}_{i \in [\mathcal{K}]}$
- 7: **else**
- 8: Update $P_{itr} = P - P_{\mathcal{K}}$.
- 9: Inference on P_{itr} with the model f_{itr-1} to calculate FS for each clip with Eq. 2,3.
- 10: Sort the clip in P in descending order of FS
- 11: Select the former n_{itr} indexes and add to \mathcal{K}
- 12: Select key frames index k for each selected clip with Eq. 4
- 13: Update $\hat{P} = \hat{P} + \{x_{i,k}, y_{i,k}\}_{i \in [\mathcal{K}]}$
- 14: **end if**
- 15: Train the model f_{itr} from scratch using \hat{P} .
- 16: **end for**

We use AdamW [Loshchilov, 2017] optimizer and Cosine Annealing [Loshchilov and Hutter,] scheduler to train VAD-Tiny with weight decay 0.01 and initial learning rate 2×10^{-4} . The approach includes the following hyper parameters: selection ratio λ set to 1/3, confidence threshold θ_τ set to 0.5, and distance threshold θ_d set to 5.0 m. We reduce EMD computation complexity by averaging the elements. VAD-Tiny is trained for 20 epochs on 8 NVIDIA GeForce RTX 4090 GPUs with batch size 1 per GPU.

4.2 Benchmark Comparison

In Tab. 1, we compare the planning performance of various algorithms under annotation budgets of 10%, 20%, and 30%, including ActiveFT [Xie *et al.*, 2023], ActiveAD [Lu *et al.*, 2024], Coreset [Sener and Savarese, 2017], and VAAL [Sinha *et al.*, 2019]. It is worth noting that the selection ratios of 20% and 30% are calculated at the clip level. Since we adopt a consecutive keyframe strategy, the actual annotation volume is lower than these values. In In [Jia *et al.*, 2024; Zhai *et al.*, 2023], the authors highlight the limitations of open-loop metrics, noting they may not reliably reflect real-world performance. Our experiments show a weak positive correlation between L2 and CR metrics, with improvements in one often accompanied by declines in the other. Therefore, when evaluating model planning performance, we consider both of these metrics comprehensively. From the table, we can see that with the VAD-Tiny model, our approach achieves performance comparable to that of the full dataset with just 30% of the annotation budget. Compared to traditional active learning algorithms, our method also demonstrates a significant performance advantage. ActiveAD is an active learning solution designed for E2E-AD, which selects data based

Table 1: Planning Performance. Comparative experimental results are referenced from [Lu *et al.*, 2024].

Base Model	Percent	Method	L2 (m) ↓				CR (%) ↓			
			1s	2s	3s	Avg.	1s	2s	3s	Avg.
ST-P3	100%	*	1.33	2.11	2.90	2.11	0.23	0.62	1.27	0.71
UniAD	100%	*	0.42	0.64	0.91	0.67	*	*	*	*
VAD-Base	100%	*	0.39	0.66	1.01	0.69	0.08	0.16	0.37	0.20
VAD-Tiny	100%	*	0.38	0.68	1.04	0.70	0.15	0.22	0.39	0.25
VAD-Tiny	10%	Random	0.51	0.83	1.23	0.86	0.40	0.62	0.98	0.67
	10%	ActiveFT	0.54	0.88	1.29	0.90	0.20	0.41	0.81	0.47
	10%	ActiveAD	0.47	0.80	1.21	0.83	0.13	0.35	0.80	0.43
	10%	SEAD(Ours)	0.50	0.80	1.17	0.82	0.13	0.25	0.53	0.30
VAD-Tiny	20%	Random	0.49	0.80	1.17	0.82	0.36	0.49	0.77	0.54
	20%	Coreset	0.48	0.78	1.16	0.81	0.20	0.40	0.69	0.43
	20%	VAAL	0.54	0.89	1.31	0.91	0.17	0.38	0.66	0.40
	20%	ActiveFT	0.50	0.82	1.21	0.84	0.27	0.42	0.63	0.44
	20%	ActiveAD	0.44	0.73	1.10	0.76	0.18	0.36	0.62	0.39
	20%	SEAD(Ours)	0.44	0.71	1.04	0.73	0.12	0.24	0.47	0.28
VAD-Tiny	30%	Random	0.45	0.76	1.12	0.78	0.17	0.30	0.63	0.37
	30%	Coreset	0.43	0.71	1.06	0.73	0.43	0.51	0.68	0.54
	30%	VAAL	0.46	0.79	1.19	0.81	0.18	0.33	0.54	0.35
	30%	ActiveFT	0.46	0.76	1.13	0.78	0.18	0.35	0.63	0.39
	30%	ActiveAD	0.41	0.66	0.97	0.68	0.10	0.18	0.36	0.21
	30%	SEAD(Ours)	0.33	0.59	0.92	0.61	0.04	0.18	0.42	0.21

Table 2: Performance comparison across different weather, lighting, and driving-command scenarios. Average L2 (m) / Average CR (%) under a 30% annotation budget are used as evaluation metrics.

Method	Weather / Lighting				Driving-Command				All
	Day	Night	Sunny	Rainy	Go Straight	Turn Left	Turn Right	Overtake	
Complete	0.67 / 0.27	1.01 / 0.14	0.70 / 0.32	0.72 / 0.04	0.69 / 0.32	0.74 / 0.13	0.67 / 0.20	0.84 / 0.13	0.70 / 0.25
Random	0.72 / 0.26	1.29 / 1.25	0.78 / 0.39	0.79 / 0.26	0.70 / 0.22	0.89 / 1.03	0.86 / 0.32	1.05 / 0.22	0.78 / 0.37
Coreset	0.71 / 0.57	0.97 / 0.27	0.72 / 0.65	0.78 / 0.06	0.69 / 0.67	0.78 / 0.31	0.78 / 0.38	0.96 / 0.14	0.73 / 0.54
VAAL	0.78 / 0.34	1.09 / 0.34	0.80 / 0.40	0.89 / 0.12	0.79 / 0.38	0.86 / 0.34	0.82 / 0.20	0.96 / 0.18	0.81 / 0.35
ActiveFT	0.76 / 0.37	1.08 / 0.43	0.79 / 0.40	0.78 / 0.28	0.70 / 0.35	0.88 / 0.62	0.91 / 0.20	1.18 / 0.44	0.79 / 0.38
ActiveAD	0.64 / 0.20	1.03 / 0.31	0.68 / 0.24	0.68 / 0.07	0.62 / 0.21	0.74 / 0.25	0.80 / 0.20	0.85 / 0.13	0.68 / 0.21
SEAD(Ours)	0.59 / 0.20	0.78 / 0.30	0.62 / 0.23	0.58 / 0.13	0.59 / 0.22	0.63 / 0.28	0.66 / 0.17	0.67 / 0.02	0.61 / 0.21

on meticulously crafted rules. In contrast, our BEV feature-based approach achieves superior planning performance with a lower annotation budget.

4.3 Ablation Study

Planning performance on fine-grained validation set

In the previous section, we noted that the AD dataset exhibits a long-tailed distribution. To mitigate the risk of overfitting the model to more common, straightforward scenarios, we subdivided the validation set based on specific driving behaviors and scenarios, following [Lu *et al.*, 2024]. This allowed us to assess the model’s performance across several distinct scenario categories, with results summarized in Tab. 2. The results show that our approach does not overfit simple scenarios and achieves competitive performance in relatively complex scenes, such as nighttime, rainy conditions, turns, and overtaking maneuvers.

Effectiveness of Modules

To evaluate the effectiveness of each module, we conduct detailed ablation experiments to systematically assess their contributions. The experimental results in Tab. 3 reveal some interesting insights. The initial selection strategy, designed based on prior information, significantly outperforms random selection in terms of performance. Besides, more data doesn’t always yield better model performance; for instance, by using selected key frames instead of entire clips, our approach achieves better collision performance while reducing the data volume.

Visualization of Selected Scenes and Frames.

The model trained on the initial dataset is used to infer on the remaining data pool. Based on predefined criteria, valuable scenes and key consecutive frames within them are selected. Some results are shown in Fig. 4.

Table 3: Effectiveness of modules. “RA” and “DS” represent random selection and initial dataset construction based on dynamic/static information, respectively. “FS” and “KF” indicate the use of feature shifts and key frames, respectively.

ID	Initiation		Active Selection		Average L2 (m)			Average CR (%)		
	RA	DS	FS	KF	10%	20%	30%	10%	20%	30%
1	✓	-	-	-	0.86	0.82	0.78	0.67	0.54	0.37
2	-	✓	-	-	0.82 (-0.04)	0.65 (-0.17)	0.67 (-0.11)	0.30 (-0.24)	0.33 (-0.04)	0.23 (-0.14)
3	-	✓	✓	-	0.82 (-0.04)	0.72 (-0.10)	0.65 (-0.13)	0.37 (-0.17)	0.32 (-0.22)	0.31 (-0.06)
4	-	✓	✓	✓	0.82 (-0.04)	0.73 (-0.09)	0.61 (-0.17)	0.30 (-0.37)	0.28 (-0.26)	0.21 (-0.16)

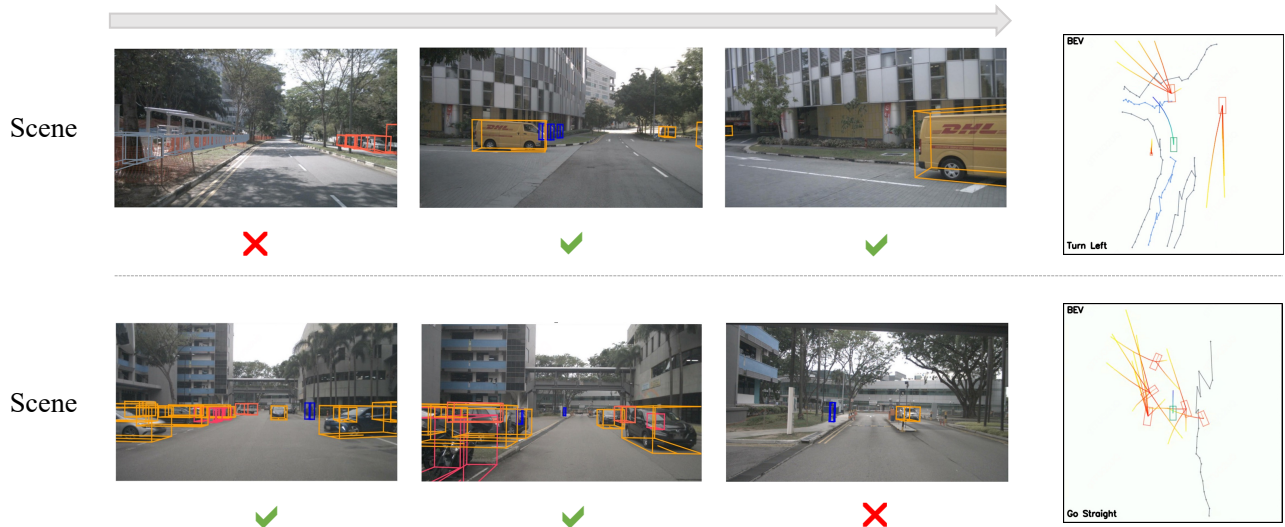


Figure 4: **Visualization of Selected Scenes and Frames.** The front camera view is used to display the selected data. The *Scene* represents a chosen scenario, with ✓ indicating the extracted key frames. BEV representation is provided to visualize the scenario value more intuitively.

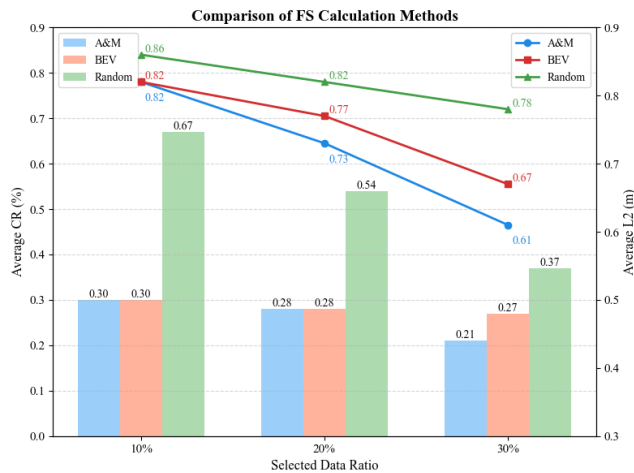


Figure 5: **Calculation of FS.** We evaluated the impact of different *FS* calculation methods on the results. Specifically, *BEV* represents *FS* calculated directly from BEV features, while *A&M* corresponds to calculations based on agent and map features.

Extension of the FS Calculation

When calculating *FS*, we begin by converting the *FS* of the entire scene to that of key elements. To further ex-

plore the robustness and versatility of this approach, we also compare it with alternative forms of *FS* calculation. The results, presented in Fig. 5, reveal that different *FS* calculation methods impact the final outcomes, though all demonstrate improved performance compared to random selection. This underscores the potential of data selection based on BEV features and the adaptability of this approach.

5 Conclusion

In this paper, we introduce SEAD, a novel active learning strategy specifically designed for E2E-AD. This approach aims to tackle two significant challenges in autonomous driving systems: the high costs associated with data labeling and the issue of long-tail distribution in driving data. Our approach selects initial data based on driving and scene diversity, while incremental data selection is guided by elemental feature offsets in BEV representations. Experimental results indicate that we achieve open-loop performance comparable to training on the entire dataset but with less than 30% of the labeling budget. Further ablation studies validate the effectiveness of each module within the framework. This work is a preliminary exploration into assessing data value from the BEV perspective, and we hope it will serve as a foundation for future research in this area.

References

- [Agarwal *et al.*, 2020] Sharat Agarwal, Himanshu Arora, Saket Anand, and Chetan Arora. Contextual diversity for active learning. In *Computer Vision–ECCV 2020: 16th European Conference, Glasgow, UK, August 23–28, 2020, Proceedings, Part XVI 16*, pages 137–153. Springer, 2020.
- [Behere and Törngren, 2015] Sagar Behere and Martin Törngren. A functional architecture for autonomous driving. In *Proceedings of the first international workshop on automotive software architecture*, pages 3–10, 2015.
- [Caesar *et al.*, 2020] Holger Caesar, Varun Bankiti, Alex H Lang, Sourabh Vora, Venice Erin Liong, Qiang Xu, Anush Krishnan, Yu Pan, Giancarlo Baldan, and Oscar Beijbom. nuscenes: A multimodal dataset for autonomous driving. In *Proceedings of the IEEE/CVF conference on computer vision and pattern recognition*, pages 11621–11631, 2020.
- [Chekroun *et al.*, 2023] Raphael Chekroun, Marin Toromanoff, Sascha Hornauer, and Fabien Moutarde. Gri: General reinforced imitation and its application to vision-based autonomous driving. *Robotics*, 12(5):127, 2023.
- [Chen *et al.*, 2020] Dian Chen, Brady Zhou, Vladlen Koltun, and Philipp Krähenbühl. Learning by cheating. In *Conference on Robot Learning*, pages 66–75. PMLR, 2020.
- [Chen *et al.*, 2024] Li Chen, Penghao Wu, Kashyap Chitta, Bernhard Jaeger, Andreas Geiger, and Hongyang Li. End-to-end autonomous driving: Challenges and frontiers. *IEEE Transactions on Pattern Analysis and Machine Intelligence*, 2024.
- [Chhabra *et al.*, 2024] Anshuman Chhabra, Peizhao Li, Prasant Mohapatra, and Hongfu Liu. ” what data benefits my classifier?” enhancing model performance and interpretability through influence-based data selection. In *The Twelfth International Conference on Learning Representations*, 2024.
- [Codevilla *et al.*, 2019] Felipe Codevilla, Eder Santana, Antonio M López, and Adrien Gaidon. Exploring the limitations of behavior cloning for autonomous driving. In *Proceedings of the IEEE/CVF international conference on computer vision*, pages 9329–9338, 2019.
- [Damianou, 2015] Andreas Damianou. *Deep Gaussian processes and variational propagation of uncertainty*. PhD thesis, University of Sheffield, 2015.
- [Elhamifar *et al.*, 2013] Ehsan Elhamifar, Guillermo Sapiro, Allen Yang, and S Shankar Sasrty. A convex optimization framework for active learning. In *Proceedings of the IEEE International Conference on Computer Vision*, pages 209–216, 2013.
- [Gal and Ghahramani, 2016] Yarin Gal and Zoubin Ghahramani. Dropout as a bayesian approximation: Representing model uncertainty in deep learning. In *international conference on machine learning*, pages 1050–1059. PMLR, 2016.
- [Gao *et al.*, 2020] Mingfei Gao, Zizhao Zhang, Guo Yu, Sercan Ö Arık, Larry S Davis, and Tomas Pfister. Consistency-based semi-supervised active learning: Towards minimizing labeling cost. In *Computer vision–ECCV 2020: 16th European conference, glasgow, UK, August 23–28, 2020, proceedings, part x 16*, pages 510–526. Springer, 2020.
- [He *et al.*, 2016] Kaiming He, Xiangyu Zhang, Shaoqing Ren, and Jian Sun. Deep residual learning for image recognition. In *Proceedings of the IEEE conference on computer vision and pattern recognition*, pages 770–778, 2016.
- [Hu *et al.*, 2022] Shengchao Hu, Li Chen, Penghao Wu, Hongyang Li, Junchi Yan, and Dacheng Tao. St-p3: End-to-end vision-based autonomous driving via spatial-temporal feature learning. In *European Conference on Computer Vision*, pages 533–549. Springer, 2022.
- [Hu *et al.*, 2023] Yihan Hu, Jiazhi Yang, Li Chen, Keyu Li, Chonghao Sima, Xizhou Zhu, Siqi Chai, Senyao Du, Tianwei Lin, Wenhai Wang, et al. Planning-oriented autonomous driving. In *Proceedings of the IEEE/CVF Conference on Computer Vision and Pattern Recognition*, pages 17853–17862, 2023.
- [Huang *et al.*, 2021] Junjie Huang, Guan Huang, Zheng Zhu, Yun Ye, and Dalong Du. Bevdet: High-performance multi-camera 3d object detection in bird-eye-view. *arXiv preprint arXiv:2112.11790*, 2021.
- [Jia *et al.*, 2024] Xiaosong Jia, Zhenjie Yang, Qifeng Li, Zhiyuan Zhang, and Junchi Yan. Bench2drive: Towards multi-ability benchmarking of closed-loop end-to-end autonomous driving. *arXiv preprint arXiv:2406.03877*, 2024.
- [Jiang *et al.*, 2023] Bo Jiang, Shaoyu Chen, Qing Xu, Bencheng Liao, Jiajie Chen, Helong Zhou, Qian Zhang, Wenyu Liu, Chang Huang, and Xinggang Wang. Vad: Vectorized scene representation for efficient autonomous driving. In *Proceedings of the IEEE/CVF International Conference on Computer Vision*, pages 8340–8350, 2023.
- [Joshi *et al.*, 2009] Ajay J Joshi, Fatih Porikli, and Nikolaos Papanikolopoulos. Multi-class active learning for image classification. In *2009 IEEE conference on computer vision and pattern recognition*, pages 2372–2379. IEEE, 2009.
- [Kiran *et al.*, 2021] B Ravi Kiran, Ibrahim Sobh, Victor Talpaert, Patrick Mannion, Ahmad A Al Sallab, Senthil Yogamani, and Patrick Pérez. Deep reinforcement learning for autonomous driving: A survey. *IEEE Transactions on Intelligent Transportation Systems*, 23(6):4909–4926, 2021.
- [Knox *et al.*, 2023] W Bradley Knox, Alessandro Allievi, Holger Banzhaf, Felix Schmitt, and Peter Stone. Reward (mis) design for autonomous driving. *Artificial Intelligence*, 316:103829, 2023.
- [Lewis and Catlett, 1994] David D Lewis and Jason Catlett. Heterogeneous uncertainty sampling for supervised learning. In *Machine learning proceedings 1994*, pages 148–156. Elsevier, 1994.
- [Li *et al.*, 2022] Zhiqi Li, Wenhai Wang, Hongyang Li, Enze Xie, Chonghao Sima, Tong Lu, Yu Qiao, and Jifeng Dai. Bevformer: Learning bird’s-eye-view representation from

- multi-camera images via spatiotemporal transformers. In *European conference on computer vision*, pages 1–18. Springer, 2022.
- [Liu *et al.*, 2021] Zhuoming Liu, Hao Ding, Huaping Zhong, Weijia Li, Jifeng Dai, and Conghui He. Influence selection for active learning. In *Proceedings of the IEEE/CVF international conference on computer vision*, pages 9274–9283, 2021.
- [Liu *et al.*, 2023] Zhijian Liu, Haotian Tang, Alexander Amini, Xinyu Yang, Huizi Mao, Daniela L Rus, and Song Han. Bevfusion: Multi-task multi-sensor fusion with unified bird’s-eye view representation. In *2023 IEEE international conference on robotics and automation (ICRA)*, pages 2774–2781. IEEE, 2023.
- [Loshchilov and Hutter,] I Loshchilov and F Hutter. Stochastic gradient descent with warm restarts. In *Proceedings of the 5th International Conference on Learning Representations*, pages 1–16.
- [Loshchilov, 2017] I Loshchilov. Decoupled weight decay regularization. *arXiv preprint arXiv:1711.05101*, 2017.
- [Lu *et al.*, 2024] Han Lu, Xiaosong Jia, Yichen Xie, Wenlong Liao, Xiaokang Yang, and Junchi Yan. Activead: Planning-oriented active learning for end-to-end autonomous driving. *arXiv preprint arXiv:2403.02877*, 2024.
- [Phillion and Fidler, 2020] Jonah Phillion and Sanja Fidler. Lift, splat, shoot: Encoding images from arbitrary camera rigs by implicitly unprojecting to 3d. In *Computer Vision—ECCV 2020: 16th European Conference, Glasgow, UK, August 23–28, 2020, Proceedings, Part XIV 16*, pages 194–210. Springer, 2020.
- [Prakash *et al.*, 2021] Aditya Prakash, Kashyap Chitta, and Andreas Geiger. Multi-modal fusion transformer for end-to-end autonomous driving. In *Proceedings of the IEEE/CVF conference on computer vision and pattern recognition*, pages 7077–7087, 2021.
- [Ren *et al.*, 2021] Pengzhen Ren, Yun Xiao, Xiaojun Chang, Po-Yao Huang, Zhihui Li, Brij B Gupta, Xiaojiang Chen, and Xin Wang. A survey of deep active learning. *ACM computing surveys (CSUR)*, 54(9):1–40, 2021.
- [Roth and Small, 2006] Dan Roth and Kevin Small. Margin-based active learning for structured output spaces. In *Machine Learning: ECML 2006: 17th European Conference on Machine Learning Berlin, Germany, September 18–22, 2006 Proceedings 17*, pages 413–424. Springer, 2006.
- [Rubner *et al.*, 2000] Yossi Rubner, Carlo Tomasi, and Leonidas J Guibas. The earth mover’s distance as a metric for image retrieval. *International journal of computer vision*, 40:99–121, 2000.
- [Sener and Savarese, 2017] Ozan Sener and Silvio Savarese. Active learning for convolutional neural networks: A core-set approach. *arXiv preprint arXiv:1708.00489*, 2017.
- [Shao *et al.*, 2023] Hao Shao, Letian Wang, Ruobing Chen, Hongsheng Li, and Yu Liu. Safety-enhanced autonomous driving using interpretable sensor fusion transformer. In *Conference on Robot Learning*, pages 726–737. PMLR, 2023.
- [Sinha *et al.*, 2019] Samarth Sinha, Sayna Ebrahimi, and Trevor Darrell. Variational adversarial active learning. In *Proceedings of the IEEE/CVF international conference on computer vision*, pages 5972–5981, 2019.
- [Tampuu *et al.*, 2020] Ardi Tampuu, Tambet Matiisen, Maksym Semikin, Dmytro Fishman, and Naveed Muhammad. A survey of end-to-end driving: Architectures and training methods. *IEEE Transactions on Neural Networks and Learning Systems*, 33(4):1364–1384, 2020.
- [Toromanoff *et al.*, 2020] Marin Toromanoff, Emilie Wirbel, and Fabien Moutarde. End-to-end model-free reinforcement learning for urban driving using implicit affordances. In *Proceedings of the IEEE/CVF conference on computer vision and pattern recognition*, pages 7153–7162, 2020.
- [Vaswani, 2017] A Vaswani. Attention is all you need. *Advances in Neural Information Processing Systems*, 2017.
- [Xie *et al.*, 2023] Yichen Xie, Han Lu, Junchi Yan, Xiaokang Yang, Masayoshi Tomizuka, and Wei Zhan. Active finetuning: Exploiting annotation budget in the pretraining-finetuning paradigm. In *Proceedings of the IEEE/CVF Conference on Computer Vision and Pattern Recognition*, pages 23715–23724, 2023.
- [Xu *et al.*, 2021] Wenda Xu, Qian Wang, and John M Dolan. Autonomous vehicle motion planning via recurrent spline optimization. In *2021 IEEE International Conference on Robotics and Automation (ICRA)*, pages 7730–7736. IEEE, 2021.
- [Zhai *et al.*, 2023] Jiang-Tian Zhai, Ze Feng, Jinhao Du, Yongqiang Mao, Jiang-Jiang Liu, Zichang Tan, Yifu Zhang, Xiaoqing Ye, and Jingdong Wang. Rethinking the open-loop evaluation of end-to-end autonomous driving in nusences. *arXiv preprint arXiv:2305.10430*, 2023.
- [Zhan *et al.*, 2022] Xueying Zhan, Qingzhong Wang, Kuanhao Huang, Haoyi Xiong, Dejing Dou, and Antoni B Chan. A comparative survey of deep active learning. *arXiv preprint arXiv:2203.13450*, 2022.
- [Zhang *et al.*, 2021] Zhejun Zhang, Alexander Liniger, Dengxin Dai, Fisher Yu, and Luc Van Gool. End-to-end urban driving by imitating a reinforcement learning coach. In *Proceedings of the IEEE/CVF international conference on computer vision*, pages 15222–15232, 2021.
- [Zhang *et al.*, 2022] Chris Zhang, Runsheng Guo, Wenyuan Zeng, Yuwen Xiong, Binbin Dai, Rui Hu, Mengye Ren, and Raquel Urtasun. Rethinking closed-loop training for autonomous driving. In *European Conference on Computer Vision*, pages 264–282. Springer, 2022.
- [Zhu *et al.*, 2020] Xizhou Zhu, Weijie Su, Lewei Lu, Bin Li, Xiaogang Wang, and Jifeng Dai. Deformable detr: Deformable transformers for end-to-end object detection. *arXiv preprint arXiv:2010.04159*, 2020.